

## Usage of vertex detectors in the ATLAS trigger software

---

**Andrea Coccaro\***

*Università degli studi di Genova and INFN Genova*

*E-mail: [Andrea.Coccaro@ge.infn.it](mailto:Andrea.Coccaro@ge.infn.it)*

### on behalf of the ATLAS collaboration

The challenging environment in which the Large Hadron Collider (LHC) experiments are going to operate implies a sophisticated trigger system, capable of real-time track and vertex reconstruction. In the ATLAS experiment, the first selection stage where these ingredients are available is the software-based High-Level Trigger (HLT), which reduces its 75 kHz input to  $\sim 200$  Hz in two subsequent steps: the LVL2 and the Event Filter (EF) triggers.

In this contribution we present algorithms for fast reconstruction of charged tracks in the HLT framework, including common extrapolation and fitting tools. Their application to different trigger selections and in particular to b-jet selections, used to improve the flexibility of the trigger scheme and extend its physics performance, is also discussed.

Examples of performance of the presented algorithms on simulation and cosmic-ray data are given. Efficient and robust tracking capabilities are demonstrated to be achievable with average execution times well within the trigger requirements.

*VERTEX 2009 (18th workshop) - VERTEX 2009*

*September 13 - 18 2009*

*Veluwe, the Netherlands*

---

\*Speaker.

## 1. Introduction

The large event rate of proton-proton collisions at the Large Hadron Collider (LHC) makes the online selection of potentially interesting physics events an essential and challenging requirement. The ATLAS experiment [1] at CERN uses a three-level trigger system to achieve the physics goals of the LHC, reducing the 40 MHz bunch crossing rate to the  $\sim 200$  Hz that can be stored permanently for physics analysis. The ATLAS detector is equipped with specialized sub-detectors to register the properties of the particles produced: its innermost part, the ATLAS tracking system also called Inner Detector, fulfills the requirement of reconstructing charged particle trajectories.

The Inner Detector (ID) consists of three independent subsystems. Nearest the beam line is the Pixel detector [2], with approximately 80 million pixels of size  $50 \times 400 \mu\text{m}$  arranged in three layers in the barrel and three end-cap wheels at large pseudorapidity values. Then, the Semiconductor Tracker (SCT) is formed by silicon micro-strips arranged in four cylindrical layers located in the barrel and nine disks in each end-cap. In the barrel region, SCT detector uses two different micro-strips with one set of strips in each layer parallel to the beam direction and a relative angle of 40 mrad. This stereoscopic geometry provides the capability to perform three-dimensional position measurements. These precision tracking detectors cover the region  $|\eta| < 2.5$  and ensure high granularity in the area around the proton-proton collisions, where a very high density of charged tracks will occur. The third tracking subsystem is the Transition Radiation Tracker (TRT) which consists of 2 mm radius straw tubes, arranged in two barrel sections with straws parallel to the beam-line direction and in two end-caps with straws arranged radially. The TRT can provide only  $R - \phi$  information, but the combination of precision trackers at small radii with the TRT gives very robust pattern recognition and high precision in both  $R - \phi$  and  $z$  coordinates. The straw hits contribute significantly to the momentum measurement, since the lower precision per point compared to silicon detectors is compensated by the large number of measurements, typically  $\sim 36$  per crossing track, and longer measured track length.

The ID is designed to reconstruct tracks with a precision of  $O(10\mu\text{m})$  in the transverse plane, achieve an excellent momentum resolution to reconstruct masses of unstable particles, measure the primary vertex to distinguish up to  $\sim 25$  primary interactions per bunch crossing expected at the design luminosity and identify secondary vertices to tag jets stemming from the hadronization of  $b$ -quarks.

## 2. The ATLAS trigger

The required reduction of event rate down to the manageable value for data storage of  $\sim 200$  Hz is provided by three subsequent trigger selection stages, where each level refines the event processing and the selection of the previous one.

The First-Level Trigger (LVL1) operates within a latency of  $2 \mu\text{s}$  and uses reduced granularity calorimeter data and dedicated muon trigger chambers. It produces a maximum output rate of 75 KHz, upgradable to 100 KHz. This trigger level also identifies Regions of Interest (ROIs) in the detector where interesting physics signatures were found. Event data of accepted events are sent out into the Data Acquisition system and further event selection is performed by software tools

running on dedicated commercial processor farms and is divided in two steps: the Second Level Trigger (LVL2) and the Event Filter (EF), collectively referred to as High-Level Triggers (HLT).

Algorithms running during the LVL2 processing have access to the detector data with the full spatial granularity, but only within the identified RoIs by LVL1. This approach reduces the data volume and processing time required for the selection and allows the handling of the LVL2 input rate. The maximum LVL2 output rate is around 3 KHz and the LVL2 decision must be taken with an average processing time of 40 ms for each event, greatly constraining the LVL2 reconstruction algorithms. LVL2 is the first stage of the ATLAS trigger system that has access to the ID data, thus specific algorithms to select events containing  $b$ -quark jets can be exploited here.

The last trigger selection stage, the EF, has much looser time constraints, of the order of 4 s, so its selections are implemented using offline analysis procedures with possible access to the complete detector data together with the full alignment and calibration.

### 3. Tracking in the LVL2 trigger

Two different silicon tracking algorithms are available for execution in the LVL2 trigger: SiTrack and IDScan.

SiTrack is a silicon hit based algorithm that implements a combinatorial approach to match space points to form full tracks. It looks for seed pairs of hits in the inner layers consistent with beam-line constraints. Pairs are then combined and extended with space points from outer layers, if matching cuts are satisfied. Groups of hits consistent with single tracks are merged and passed to the track fitter.

IDScan is also a silicon hit based algorithm that exploits a space point histogramming method. The determination of the  $z$  position of the interaction point along the beam axis is the first required step, needed to identify clusters of hits in  $\eta - \phi$  space. Then, groups of hits from these clusters that are consistent in  $1/p_T - \phi$  space are passed to the track fitter.

After the pattern recognition stage performed by SiTrack and IDScan, both algorithms share a common Kalman filter track fit for fast track reconstruction. Moreover, tracks can be extrapolated using the TRT information to improve  $p_T$  resolution and particle identification.

The approach adopted for the EF tracking, given the more relaxed timing requirements, is based on reusing as much as possible the code developed for offline reconstruction. Anyway, to deal with the minor processing time allowed at the EF level, some adaptations with respect to offline reconstruction are mandatory. Thus, the offline code is executed within wrapper algorithms, which can access only data contained in the RoIs (with the exception of specific  $B$ -physics driven signatures). Moreover, additional tunings of algorithm parameters can be performed to reduce the number of iterations or to skip part of the reconstruction process.

HLT tracking is widely used in the definition of the most crucial trigger objects: selection of high- $p_T$  electrons and muons, track reconstruction from tau decays, reconstruction of exclusive decays for identification of specific  $B$ -physics channels and  $b$ -jet tagging. The latter trigger selection is described in details in section 4.

These algorithms are obviously designed and optimized for a collision scenario where tracks are originating from the beam line with relatively small impact parameters. For the cosmic data-taking, a different strategy has been instrumented to cope with the different event topology since

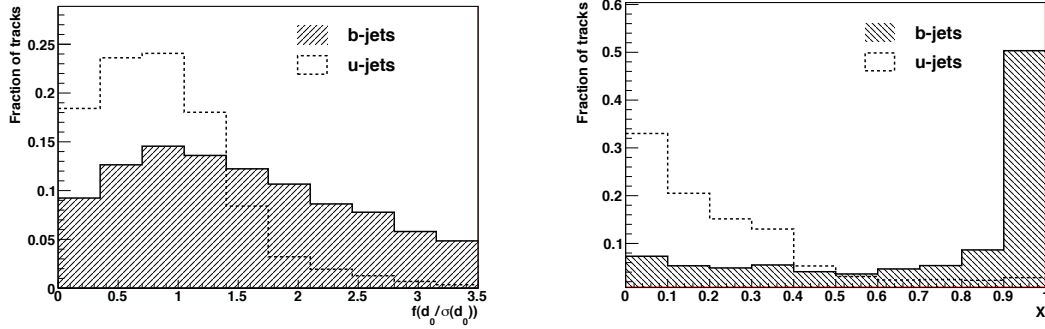


**Figure 1:** Distribution of the transverse impact parameter significance for tracks coming from  $b$ -jets and  $u$ -jets on the left and corresponding discriminant distribution on the right, using a  $t\bar{t}$  Monte Carlo sample at a center-of-mass-energy of 14 TeV.

cosmic tracks can pass significantly far away from the beam line in the transverse plane. These modified LVL2 tracking algorithms were used to select, with high purity, events where the cosmic muons went through the ID and were subsequently analyzed for ID alignment and offline performance studies. Details and corresponding LVL2 tracking performance are given in section 5 of this contribution.

EF tracking was also deployed during cosmic operations but it was not used to effectively select events. Results of EF tracking performance with cosmic data are not presented in this contribution.

#### 4. Online $b$ -tagging

The online selection of  $b$ -jets is mainly meant to improve the flexibility of the HLT, extending its physics performance for events with final states containing several  $b$ -jets. This is achieved by increasing the acceptance for signal events at low momenta, while lowering the background. The most promising channels which benefit from requesting this kind of trigger firing are the  $H \rightarrow b\bar{b}$  decay, where the Higgs boson is produced by way of the associated production channel  $t\bar{t}H$  and, in supersymmetric theories, the channels  $b\bar{b}H$ ,  $b\bar{b}A$  with  $H/A \rightarrow b\bar{b}$  or  $H \rightarrow hh \rightarrow b\bar{b}b\bar{b}$ .

The HLT reconstruction starts from the RoIs selected by the LVL1 trigger. In particular, the  $b$ -jet signatures are activated starting from a LVL1 jet RoI with dimensions equal to 0.8 in  $\eta$  and  $\phi$ . At LVL2, track and vertex reconstruction is performed in a smaller RoI, half size in  $\eta$  and  $\phi$ , in order to reduce data access and consequently processing time. Presently, the primary vertex is estimated only in the beam-line direction while its coordinates in the transverse plane are assumed to be compatible with the beam spot position. After track and vertex reconstruction, discriminant  $b$ -tagging variables are estimated and a selection criterion is applied. The EF  $b$ -tagging selection is run only if the LVL2 decision is positive.

$b$ -jet tagging algorithms included in the ATLAS trigger selection exploit the transverse and longitudinal signed impact parameter distribution of reconstructed tracks. The sign is the result of the dot product of the jet axis direction and the line connecting the primary vertex position to the

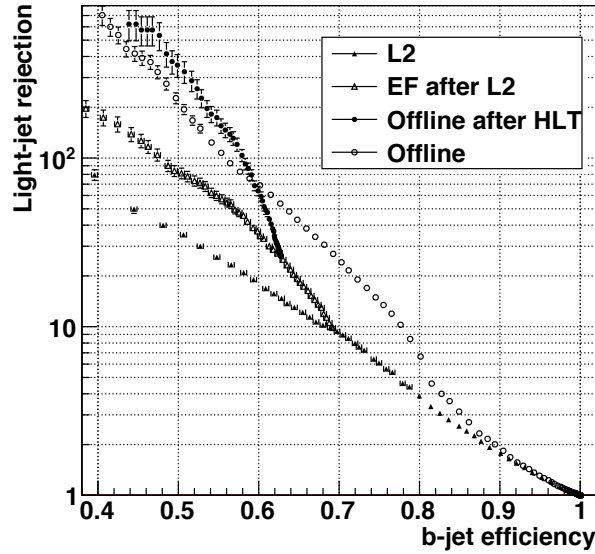


**Figure 2:**  $b$ -jet performance at LVL2 and EF, where the EF selection starts from the chosen L2 working point, for the two-dimensional combination of the track signed impact parameters. The  $b$ -tagging correlation between online and offline is also shown.

point of closest approach of the track to the beam line. New  $b$ -jet tagging algorithms based on the secondary vertex reconstruction and its properties are currently being studied and they will be first deployed at the EF level.

Most of the available algorithms implement a *likelihood-ratio* approach. The *likelihood-ratio* variable  $W$  is evaluated as the ratio between the probability density distributions for the two alternative hypothesis: the signal ( $b$ -jets) and the background (light-quark jets).

The  $W$  variable is estimated using all the reconstructed tracks which fulfill specific selection criteria:

$$W = \prod_{i=1}^{N_{\text{tracks}}} \frac{P_b(S_i)}{P_u(S_i)} \quad (4.1)$$

where  $P_b$  and  $P_u$  are the probability densities for the signal and the background while  $S$  is a function of track parameters that can be one of the following variables: longitudinal impact parameter significance, transverse impact parameter significance and the two-dimensional combination of the previous significances. The latter, combining more physics information, produces the best performance relative to each of the other two methods and to the direct product of the two different one-dimensional algorithms since, in this way, correlations between longitudinal and transverse impact parameters are taken into account. The  $W$  variable can take any value between 0 and  $+\infty$ , with the signal generally distributed at higher values than the background. To handle a variable defined on a finite interval,  $W$  is replaced by a new variable  $X = W/(W + 1)$ , so that signal events accumulate near  $X = 1$  while the background tends to have  $X \sim 0$ . Figure 1 depicts the two differ-

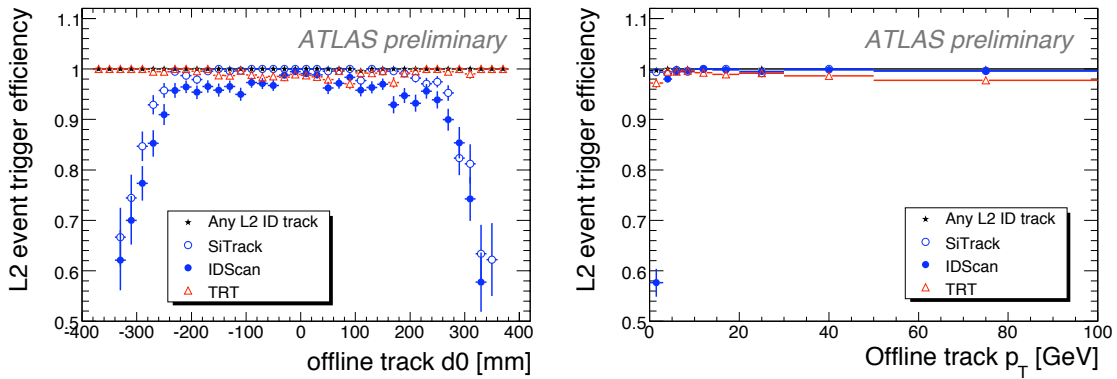


**Figure 3:** The LVL2 event finding efficiency for good offline tracks versus the reconstructed transverse impact parameter  $d_0$  of offline tracks (on the left) and versus the reconstructed transverse momentum  $p_T$  of offline tracks (on the right).

ent distributions based on the transverse impact parameter significance for  $b$ -jets and  $u$ -jets in a  $t\bar{t}$  Monte Carlo sample at a center-of-mass-energy of 14 TeV and the corresponding  $X$  variable.

The  $b$ -tagging performance is characterized by the curve showing the light-quark jet rejection versus the efficiency for selecting  $b$ -jets. The light-quark jet rejection is defined as the inverse of the efficiency for selecting  $u$ -jets ( $u$ -jets are assumed as representative of general light-quark jets). Figure 2 depicts the HLT  $b$ -tagging performance using both the transverse and longitudinal impact parameter significances in a  $t\bar{t}$  Monte Carlo sample. The performance of the corresponding offline algorithm is also shown in the same plot.

Figure 2 demonstrates that online and offline selections are well correlated since the full offline performance at a given  $b$ -jet efficiency can be completely recovered if the LVL2 and EF working points are set at an appropriate higher efficiency. The  $b$ -tagging efficiencies shown in figure 2 are  $\varepsilon_b = 70(63)\%$  for the LVL2(EF) selection, ensuring nominal performance for the analogous offline tagger at  $\varepsilon_b = 60\%$ , which is the usual offline working point.

## 5. Tracking performance with cosmic rays

From September to December 2008, the ATLAS detector recorded more than 200 million cosmic muons as part of a campaign to commission as many aspects of the experiment as possible while waiting for the LHC repair to proceed. This large data set, together with the use of the entire infrastructure to deal with condition and calibration data, have allowed to apply detailed alignment corrections during two major reprocessing campaigns. Efficiency studies using 2008 cosmic reprocessed data are presented in this section. Other cosmic data-taking periods occurred in 2009, specifically in June and starting from November until the LHC turn on, foreseen by the end of the year. More detailed studies on HLT tracking performance are presently underway.

To deal with the different event topology, the two silicon based tracking algorithms adopted a different strategy. SiTrack was operational with relaxed beam-line constraints while IDScan used an additional pre-processing stage, specifically devoted for cosmic tracks reconstruction, to shift the space points as if they were coming from the interaction region.

Besides the LVL2 silicon tracking algorithms, an ad-hoc algorithm to reconstruct cosmic tracks using only hits from the TRT detector was in place. It is a wrapped version of the offline tracking, limiting its search window in  $\phi$  to about  $\pm 45^\circ$  from the vertical direction, called TRT Segment Finder.

The L2 event reconstruction efficiency for 2008 cosmic data is shown in this section for the three different tracking algorithms since they were all used to stream events and thus providing a sample with tracks illuminating as much as possible the ID. This sample was then used to derive an early set of alignment constants for the ID before the LHC start up [3]. The LVL2 efficiency is defined with respect to an event with an offline track with at least three silicon space points in the upper and three in the lower part of the silicon barrel. Either of the two track arms can be independently reconstructed by the LVL2 silicon-based algorithms. If there is more than one such track in an event, the track with the most hits in common with the offline track is retained.

The left plot of figure 3 depicts the event finding efficiency for events with a good offline cosmic track as a function of the offline transverse impact parameter  $d_0$ . The larger size of the TRT detector results in a flat distribution in  $d_0$  for the TRT Segment Finder and a very good performance up to very large impact parameter values is achieved. For the silicon algorithms, the efficiency starts to fall at about 250 mm because pixel hits are not present anymore and first hits from the inner layers of SCT are lost as well. The lower IDScan efficiency with respect to SiTrack is understood by studying the corresponding efficiency as a function of the transverse momentum  $p_T$  of the reconstructed offline track, depicted in the right plot of figure 3. Here, the IDScan inefficiency is clearly in the lowest  $p_T$  bin. This efficiency loss is due to the pre-processor stage, when space points are shifted. Since it uses a straight track fit to estimate the impact parameter and shift the space points accordingly, this method is less accurate whenever the track presents a significant curvature. The efficiency for SiTrack and IDScan at higher  $p_T$ , when the space-point shifter performs well, is otherwise comparable.

The combined efficiency for all three algorithms is better than 99% for all cosmic muons passing through the ID barrel volume and is almost 100% when considering high  $p_T$  tracks. Fake rate contribution was also evaluated using events from random triggers where no cosmic tracks are expected and for all the three algorithms the fake tracks were well below 1%, perfectly acceptable for cosmic data taking.

During the cosmic data-taking period, different operational configurations were tested, in particular with and without the solenoidal magnetic field. Results shown in this contribution are with magnetic field on since this is the scenario for collecting physics data.

## 6. Conclusions

An overview of the different tracking approaches available for the online selection of the ATLAS experiment was presented in this report. A more detailed description of the online  $b$ -jet tagging, the ingredient in the ATLAS trigger which accesses detailed informations only from the tracking subsystems, was also given. Results, based on Monte Carlo studies, highlight that this selection can play an important role in the ATLAS physics programme especially for events with multiple  $b$ -jets where very high rejection factors are achieved, allowing a significant decrease of the LVL1 thresholds while keeping the output rate of LVL2 and EF almost constant.

Moreover the usage of different LVL2 tracking algorithms during the 2008 cosmic data-taking period was described. An efficiency of nearly 100% was achieved using the combination of the available tracking algorithms at the second trigger level and the collected sample has been successfully used for detector alignment and further offline studies.

## **7. Acknowledgments**

The author would like to acknowledge the ATLAS High-Level Trigger community for all the direct and indirect contributions to the work presented here and thanks the workshop organizers for the invitation and the very interesting programme.

## **References**

- [1] The ATLAS Collaboration, The ATLAS Experiment at the CERN Large Hadron Collider, JINST 3 S08003, 2008.
- [2] G. Aad et al, ATLAS pixel detector electronics and sensors, JINST 3 P07007, 2008.
- [3] Heather M. Gray, Alignment of the ATLAS inner detector tracking system, JINST 4 P03018, 2009.